Orientation and Restricted Rotation of Lopsided Aromatic Ligands. Octahedral Complexes Derived from *cis*-$RuCl_2(Me_2SO)_4$

Enzo Alessio,[†] Mario Calligaris,[†] Marian Iwamoto,[‡] and Luigi G. Marzilli*,[‡]

Department of Chemistry, Emory University, Atlanta, Georgia 30322,
and Dipartimento di Scienze Chimiche, Università di Trieste, Trieste, Italy

Received July 29, 1995[⊗]

The solution and solid state structures of two octahedral Ru(II) complexes, *cis*,*cis*,*cis*-$RuCl_2(Me_2SO)_2(py)(Me_3Bzm)$ (Me_3Bzm = 1,5,6-trimethylbenzimidazole, py = pyridine) (**1**) and *cis*,*cis*,*cis*-$RuCl_2(Me_2SO)_2(Me_3Bzm)_2$ (**2**), were compared. **2**, the subject of a preliminary report, is described in more detail here. **1** has two possible geometric isomers with py *trans* to Cl in one (position "a") and *trans* to Me_2SO in the other (position "b"), Me_3Bzm occupying the other position in each isomer. The X-ray structure of **1** revealed that py is at "a". Since Me_3Bzm is lopsided, each Me_3Bzm has two possible orientations related by a rotation of ∼180° about the Ru−N3 bond; there are two possible atropisomers for each geometric isomer of **1** and four for **2**. For **1**, the solid state structure shows that Me_3Bzm adopts the orientation with H2 (H on C between the two N's) pointing between the two *cis* Cl ligands, the same disposition as Me_3Bzm "b" in **2** in the solid. For **1**, the py signals (two broad py α and β signals, a sharp γ signal) in $CDCl_3$ show that py "a" is rotating on the NMR time scale and that only one atropisomer is present. This interpretation was supported by ROESY and EXSY ^1H NMR spectra. The ^1H NMR shift pattern and the NOE data can be understood best if Me_3Bzm "b" remains primarily in the orientation found in the solid. The solution data for **1**, with the nonlopsided and sterically less demanding py ligand, provide insight into the more complicated properties of **2**. For **2**, there is a marked dispersion of ^1H NMR signals of Me_3Bzm "a" between the two atropisomers, which have nearly equal stability. One atropisomer is a head-to-head (HH) and the other a head-to-tail (HT) species. Me_3Bzm "a" flips between the two species. Thus, ligand "a" is fluxional in both complexes. The dispersion of Me_3Bzm "a" signals is due to the effect of Me_3Bzm "b" anisotropy. For **1** and both atropisomers of **2**, Me_3Bzm "b" prefers one orientation, which appears to be the most hindered orientation. We postulate that the H2 of Me_3Bzm "b" is electrostatically attracted to the two *cis* halides, accounting for this surprising result. Crystallographic details for **1** are as follows: $C_{19}H_{29}Cl_2N_3O_2RuS_2$, $P2_1/c$, a = 10.947(1) Å, b = 9.046(1) Å, c = 24.221(2) Å, D(calcd) = 1.580 g cm^{-3}, Z = 4, R = 0.026 for 4627 independent reflections.

Introduction

The majority of stereodynamic processes that have been investigated in the field of inorganic chemistry concern fluxional isomerism in systems with π-bound ligands and scrambling in carbonyl clusters.[1,2] Surprisingly, despite extensive studies devoted to the rotation of coordinated π-systems,[1−6] the topic of restricted rotation about the metal−ligand σ bond in simple coordination compounds has escaped investigation except in square planar complexes.

Examples of these square planar complex studies found in the literature deal mainly with the mechanism of action of platinum(II) analogues of the anticancer drug cisplatin (*cis*-$PtCl_2(NH_3)_2$). Well-documented cases of restricted rotation about Pt−N(nucleoside) bonds were first presented by Cramer[7] and were later investigated in detail by other groups.[8−16] A dependence of the nucleoside rotation rate on the bulkiness of the nonlabile amine ligands and of the nucleoside itself[13] was established.

An example of hindered rotation about metal−phosphorus bonds has been reported for a square planar Rh(I) complex with bulky phosphines.[17] Another particularly well-studied example concerns hindered rotation of dialkylamido ligands in some four-coordinate molybdenum dimers where, however, the Mo−NR_2 bond has a partial double-bond character.[18,19]

Nuclear magnetic resonance (NMR) spectroscopy is a powerful tool for investigating degenerate (topomerization) and nondegenerate (diastereotopomerization) stereodynamic pro-

[†] Università di Trieste.
[‡] Emory University.
[⊗] Abstract published in *Advance ACS Abstracts,* March 15, 1996.

(1) Orrell, K. G.; Sik, V. *Annu. Rep. NMR Spectrosc.* **1987**, *19*, 79.
(2) Perrin, C. L.; Dwyer, T. J. *Chem. Rev.* **1990**, *90*, 935.
(3) Albright, T. A. *Acc. Chem. Res.* **1982**, *15*, 149.
(4) Wickenheiser, E. B.; Cullen, W. R. *Inorg. Chem.* **1990**, *29*, 4671.
(5) Carmona, E.; Hughes, A. K.; Muñoz, M. A.; O'Hare, D. M.; Pérez, P. J.; Poveda, M. L. *J. Am. Chem. Soc.* **1991**, *113*, 9210.
(6) Gallop, M. A.; Johnson, B. F. G.; Keeler, J.; Lewis, J.; Heyes, S. J.; Dobson, C. M. *J. Am. Chem. Soc.* **1992**, *114*, 2510.
(7) Cramer, R. E.; Dahlstrom, P. L. *J. Am. Chem. Soc.* **1979**, *101*, 3679.
(8) Marcelis, A. T. M.; van der Veer, J. L.; Zwetsloot, J. C. M.; Reedijk, J. *Inorg. Chim. Acta* **1983**, *78*, 195.
(9) Marcelis, A. T. M.; Erkelens, C.; Reedijk, J. *Inorg. Chim. Acta* **1984**, *91*, 129.
(10) Lempers, E. L. M.; Bloemink, M. J.; Reedijk, J. *Inorg. Chem.* **1991**, *30*, 201.
(11) Inagaki, K.; Dijt, F. J.; Lempers, E. L. M.; Reedijk, J. *Inorg. Chem.* **1988**, *27*, 382.
(12) Reily, M. D.; Wilkowski, K.; Shinozuka, K.; Marzilli, L. G. *Inorg. Chem.* **1985**, *24*, 37.
(13) Reily, M. D.; Marzilli, L. G. *J. Am. Chem. Soc.* **1986**, *108*, 6785.
(14) Xu, Y.; Natile, G.; Intini, F. P.; Marzilli, L. G. *J. Am. Chem. Soc.* **1990**, *112*, 8177.
(15) Sundquist, W. I.; Bancroft, D. P.; Lippard, S. J. *J. Am. Chem. Soc.* **1990**, *112*, 1590.
(16) Kiser, D.; Intini, F. P.; Xu, Y.; Natile, G.; Marzilli, L. G. *Inorg. Chem.* **1994**, *33*, 4149.
(17) Bushweller, C. H.; Hoogasian, S.; English, A. D.; Miller, J. S.; Lourandos, M. Z. *Inorg. Chem.* **1981**, *20*, 3448.
(18) Chisholm, M. H.; Folting, K.; Huffman, J. C.; Rothwell, I. P. *Organometallics* **1982**, *1*, 251.
(19) Coffindaffer, T. W.; Westler, W. M.; Rothwell, I. P. *Inorg. Chem.* **1985**, *24*, 4565.

0020-1669/96/1335-2538$12.00/0

Chart 1. Numbering Scheme and Intraligand NOE Connectivity Path for the Me_3Bzm Ligand[a]

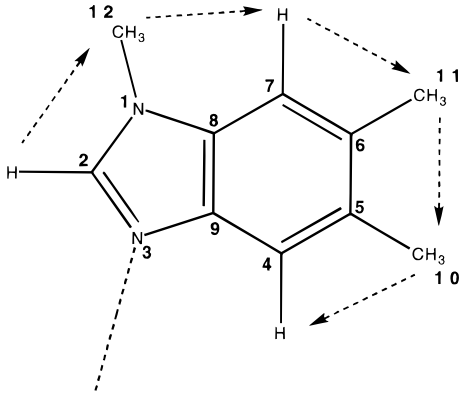

[a] The carbons are designated as "B" (for benzimidazole) in the references to NMR results in the text.

cesses[20] in chemical systems and for the determination of associated kinetic parameters (dynamic NMR).[21] In general, slow rotation on the NMR time scale by some ligands lowers the symmetry of the complex (particularly when the ligands are lopsided); lower symmetry enhances the opportunity for structural assignment by NMR spectroscopy. The number of signals will depend on the symmetry of the complex, on the local symmetry of the ligands involved in the process, on their rate of rotation, and on the frequency dispersion in the static spectrum of the nuclei undergoing exchange. In the case of square planar complexes, a detailed study on the number of resonances expected for each type of observable nucleus has been reported.[12] However, the complexity of the system rapidly increases with the coordination number, making higher coordination complexes potentially more difficult to study.

In this paper, we report an extensive investigation of two octahedral complexes, *cis*,*cis*,*cis*-$RuCl_2(Me_2SO)_2(py)(Me_3Bzm)$ (**1**) and *cis*,*cis*,*cis*-$RuCl_2(Me_2SO)_2(Me_3Bzm)_2$ (**2**), in which rotation of the nitrogen ligands about the Ru−N bond is restricted at room temperature [Me_3Bzm = 1,5,6-trimethylbenzimidazole (Chart 1); py = pyridine; Me_2SO = S-bonded dimethyl sulfoxide (DMSO)]. Complex **1** provides an example of topomerization, while **2** is a good example of diastereotopomerization. (A brief description of the structure of **2** has appeared as a Communication.[22]) Planar py and Me_3Bzm were chosen as examples of C_2-symmetric and non-C_2-symmetric (lopsided) ligands, respectively. Lopsided ligands, such as benzimidazole, substituted imidazoles, and nucleobases, are good models for the metal-bonding units of biologically relevant molecules and biopolymers. Moreover, the protons in Me_3Bzm are not coupled, greatly simplifying the interpretation of NMR spectra obtained from two-dimensional (2D) NMR techniques such as exchange correlation spectroscopy (EXSY)[1,23−25] and rotating-frame Overhauser enhancement spectroscopy (ROESY).[26−28]

This work has also been stimulated by our interest in the chemistry of ruthenium−sulfoxide complexes;[29] these have promising antitumor and, in particular, antimetastatic properties.[30] Since the mechanism of action of ruthenium complexes is believed to involve the interaction with the nucleobases of DNA,[31−33] we are actively investigating the reactions of ruthenium−sulfoxide complexes with model nitrogen donor ligands.[34,35] Previous work on interactions of ruthenium−sulfoxide complexes with mononucleotides has already shown that these complexes can produce geometrical diastereomeric products.[36] The evidence reported here for the rather facile formation of diastereoisomers that differ in the conformation of the Me_3Bzm ligands confirms the higher degree of complexity of octahedral complexes compared to square planar derivatives.

Experimental Section

Physical Measurements. Electronic absorption spectra were recorded in stoppered quartz cells with a Cary 3 spectrophotometer equipped with a thermostated cell compartment. Elemental analyses were performed by Atlantic Microlabs, Atlanta, GA.

IR Spectroscopy. IR spectra were collected on samples pressed into KBr pellets, on a Perkin-Elmer 983G spectrometer. Spectra are reported in reciprocal centimeters.

NMR Spectroscopy. ^{1}H NMR experiments were performed either at 361.10 MHz on a GE NT-360 spectrometer or at 599.64 MHz on a GE GN-600 Omega spectrometer. Sample concentrations varied from 30 to 100 mM, depending on compound solubility; solvents used included $CDCl_3$, CD_2Cl_2, CD_3COCD_3, and DMSO-d_6. All spectra were referenced to TMS.

(a) One-Dimensional (1D) ^{1}H NMR Spectroscopy. Spectra were typically collected with a 4500−7000 Hz spectral window, a 30° pulse width, and 16K data points. Variable-temperature (VT) studies were performed on the NT-360 from −80 to +50 °C. NOE difference spectra were collected on the GN-600 Omega spectrometer; 240 scans were collected with the saturating field directed off resonance and subtracted from an equal number of scans with the saturating field on resonance. Spectra were collected with 16K data points zero-filled to 64K.

(b) 2D ^{1}H−^{1}H EXSY. The proton 2D EXSY experiment[1,23−25] was performed on the NT-360. A 512 × 1024 data matrix was collected with 32 scans per t_1 increment. Each acquisition was preceded by four dummy scans and a 1-s relaxation delay. A mixing time of 750 ms was implemented along with a 3846.15 Hz spectral window. The data were processed in an absolute-value mode with Felix 1.1 (Hare Research, Inc., Woodinville, WA) on an SGI 4D/25 Personal Iris Computer. A square sine bell filter with no phase shift was applied in both dimensions. The second dimension was zero-filled to 1024 data points prior to Fourier transformation.

(c) 2D ^{1}H−^{1}H ROESY. The homonuclear hypercomplex 2D ^{1}H ROESY experiment[26−28] was performed on the GN-600 Omega spectrometer. A 512 × 2048 data matrix was collected with 32 scans per t_1 increment. The spectrometer frequency was set off-center, downfield. A 14 285.71 Hz window was used along with a spin lock

(20) Kessler, H. *Angew. Chem., Int. Ed. Engl.* **1970**, *9*, 219.
(21) Sandström, J. *Dynamic NMR Spectroscopy*; Academic Press: London, 1982.
(22) Marzilli, L. G.; Iwamoto, M.; Alessio, E.; Hansen, L.; Calligaris, M. *J. Am. Chem. Soc.* **1994**, *116*, 815.
(23) Jeener, J.; Meier, B. H.; Bachmann, P.; Ernst, R. R. *J. Chem. Phys.* **1979**, *71*, 4546.
(24) Kumar, A.; Ernst, R. R.; Wüthrich, K. *Biochem. Biophys. Res. Commun.* **1980**, *95*, 1.
(25) States, D. J.; Haberkorn, R. A.; Ruben, D. J. *J. Magn. Reson.* **1982**, *48*, 286.
(26) Bothner-By, A. A.; Stephens, R. L.; Lee, J.-m.; Warren, C. D.; Jeanloz, R. W. *J. Am. Chem. Soc.* **1984**, *106*, 811.
(27) Bax, A.; Davis, D. G. *J. Magn. Reson.* **1985**, *63*, 207.
(28) Griesinger, C.; Ernst, R. R. *J. Magn. Reson.* **1987**, *75*, 261.
(29) Alessio, E.; Sessanta o Santi, A.; Faleschini, P.; Calligaris, M.; Mestroni, G. *J. Chem. Soc., Dalton Trans.* **1994**, 1849.
(30) Mestroni, G.; Alessio, E.; Sava, G.; Pacor, S.; Coluccia, M.; Boccarelli, A. *Met.-Based Drugs* **1994**, *1*, 41.
(31) Mestroni, G.; Alessio, E.; Sava, G.; Pacor, S.; Coluccia, M. In *Metal Complexes in Cancer Chemotherapy*; Keppler, B. K., Ed.; VCH Verlag: Weinheim, Germany, 1993; p 157.
(32) Clarke, M. J.; Jansen, B.; Marx, K. A.; Kruger, R. *Inorg. Chim. Acta* **1986**, *124*, 13.
(33) Loseto, F.; Alessio, E.; Mestroni, G.; Lacidogna, G.; Nassi, A.; Giordano, D.; Coluccia, M. *Anticancer Res.* **1991**, *11*, 1549.
(34) Henn, M.; Alessio, E.; Mestroni, G.; Calligaris, M.; Attia, W. M. *Inorg. Chim. Acta* **1991**, *187*, 39.
(35) Iwamoto, M.; Alessio, E.; Marzilli, L. G. *Inorg. Chem.*, in press.
(36) Alessio, E.; Xu, Y.; Cauci, S.; Mestroni, G.; Quadrifoglio, F.; Viglino, P.; Marzilli, L. G. *J. Am. Chem. Soc.* **1989**, *111*, 7068.

Table 1. Summary of Crystal Data, Data Collection Parameters, and Structure Refinement for *cis,cis,cis*-$RuCl_2(Me_2SO)_2(py)(Me_3Bzm)$ (**1**)

mol formula	$C_{19}H_{29}Cl_2N_3O_2RuS_2$
fw	567.55
cryst system	monoclinic
space group	$P2_1/c$
a, Å	10.947(1)
b, Å	9.046(1)
c, Å	24.221(2)
β, deg	95.72(1)
V, Å^3	2386(1)
Z	4
D(calcd), g cm^{-3}	1.580
μ(Mo Kα), cm^{-1}	10.6
cryst size, mm	0.2 × 0.3 × 0.6
transm factors	0.969−0.998
radiation	graphite-monochromated Mo Kα (λ = 0.7107 Å)
scan type	$\omega/2\theta$
θ range, deg	2−28
scan speed, deg min^{-1}	1−20
scan range, deg in ω[a]	0.70 + 0.35 tan θ
aperture width, mm	1.00 + tan θ
no. of intensity monitors[b]	3
no. of collected data ($\pm h,+k,+l$)	6238
unique data with $I > 3\sigma(I)$	4627
final no. of variables	263
R[c]	0.026
R_w[d]	0.027
w	1
GOF[e]	0.966
$\Delta(\rho)$, e Å^{-3}	−0.45, 0.54

[a] Extended by 25% on both sides for background measurements. [b] Measured every 83 min. [c] $R = \sum(||F_o| - |F_c||)/\sum|F_o|$. [d] $R_w = [\sum w(|F_o| - |F_c|)^2/\sum w|F_o|^2]^{1/2}$. [e] GOF = $[\sum w(|F_o| - |F_c|^2)/(m - n)]^{1/2}$; m = number of observations, n = number of variables.

field of 3125 Hz with a 500-ms duration. A 1.5-s relaxation delay was incorporated prior to each scan, and the entire experiment was preceded by four dummy scans. The data were processed in a phase-sensitive absorption mode using an exponential multiplication with a line broadening of 1 Hz in the t_2 dimension. The second dimension was zero-filled to 2048 data points, and a 90° shifted square sine bell filter was applied to the first 512 data points prior to Fourier transformation.

Crystallographic Measurements. Suitable crystals of *cis,cis,cis*-$RuCl_2(Me_2SO)_2(py)(Me_3Bzm)$, **1**, were obtained by recrystallization of the crude product from chloroform/DMSO mixtures upon addition of diethyl ether. Diffraction measurements were carried out on an Enraf-Nonius CAD-4 fully automated diffractometer. Cell parameters were refined from 25 randomly selected reflections by using the CAD-4 automated routines. Crystal data and data collection parameters are listed in Table 1. All data processing was performed on a MicroVAX-2000 computer using the MolEN program library.[37] Neutral-atom scattering factors and anomalous dispersion terms for non-hydrogen atoms were taken from the literature.[38]

The structure was solved by the heavy-atom method. Hydrogen atoms were located at calculated positions (C−H = 0.95 Å) and held fixed (B = 1.3(B_{eq} of the attached atom)) during refinement. Full-matrix least-squares refinement with anisotropic thermal parameters for all the refined atoms converged to the final R factor shown in Table 1. Atomic parameters of **1** appear in Table 2, and selected bond distances and angles appear in Table 3.

Reagents. DMSO, pyridine, and all the other solvents (Fisher) were used without further purification. All other reagents were from Aldrich. Deuterated solvents were purchased from Aldrich and Cambridge Isotope Laboratories.

Table 2. Positional Parameters and Estimated Standard Deviations for *cis,cis,cis*-$RuCl_2(Me_2SO)_2(py)(Me_3Bzm)$ (**1**)

atom	x	y	z	B_{eq}[a] Å^2
Ru	0.18941(1)	0.21457(2)	0.10883(1)	2.537(3)
Cl1	0.00668(5)	0.35912(9)	0.08398(3)	4.64(1)
Cl2	0.18153(6)	0.13135(8)	0.01346(2)	4.27(1)
S1	0.08194(5)	0.01311(8)	0.13029(2)	3.50(1)
S2	0.19415(5)	0.31232(7)	0.19460(2)	3.33(1)
O1	0.0979(2)	−0.0382(3)	0.18853(8)	5.55(5)
O2	0.2927(2)	0.2703(2)	0.23795(7)	4.27(4)
N1	0.3529(2)	0.0918(2)	0.12536(8)	2.92(3)
N2	0.2916(2)	0.3976(2)	0.08344(8)	2.87(3)
N3	0.3361(2)	0.5859(2)	0.02978(8)	3.06(4)
C1	0.1094(3)	−0.1455(4)	0.0898(1)	5.21(7)
C2	−0.0794(2)	0.0292(4)	0.1120(1)	4.87(6)
C3	0.0546(3)	0.2891(5)	0.2258(1)	5.71(8)
C4	0.1976(4)	0.5090(4)	0.1921(1)	5.88(8)
C5	0.4357(2)	0.0855(3)	0.0878(1)	3.37(5)
C6	0.5472(2)	0.0142(3)	0.0983(1)	4.36(6)
C7	0.5762(3)	−0.0537(4)	0.1483(1)	4.93(6)
C8	0.4926(3)	−0.0503(3)	0.1863(1)	4.64(6)
C9	0.3827(2)	0.0224(3)	0.1739(1)	3.76(5)
C10	0.2521(2)	0.4857(3)	0.04173(9)	3.08(4)
C11	0.3201(3)	0.7000(3)	−0.0126(1)	3.79(5)
C12	0.4400(2)	0.5607(3)	0.06572(9)	2.86(4)
C13	0.5562(2)	0.6260(3)	0.0704(1)	3.33(4)
C14	0.6436(2)	0.5732(3)	0.1106(1)	3.27(4)
C15	0.7712(2)	0.6378(3)	0.1155(1)	4.46(6)
C16	0.7115(2)	0.3969(4)	0.1889(1)	4.41(6)
C17	0.6145(2)	0.4578(3)	0.14654(9)	3.14(4)
C18	0.4989(2)	0.3944(3)	0.14165(9)	2.97(4)
C19	0.4117(2)	0.4444(3)	0.09970(9)	2.70(4)

[a] Anisotropically refined atoms are given in the form of the isotropic eqivalent displacement parameter defined as (4/3)[$a^2\beta$(1,1) + $b^2\beta$(2,2) + $c^2\beta$(3,3) + ab(cos γ)β(1,2) + ac(cos β)β(1,3) + bc(cos α)β(2,3)].

Table 3. Selected Bond Distances (Å) and Angles (deg) for *cis,cis,cis*-$RuCl_2(Me_2SO)_2(py)(Me_3Bzm)$ (**1**)

Ru−Cl1	2.4148(7)	S1−O1	1.479(2)
Ru−Cl2	2.4233(6)	S1−C1	1.781(3)
Ru−S1	2.2576(7)	S1−C2	1.783(3)
Ru−S2	2.2541(6)	S2−O2	1.478(2)
Ru−N1	2.110(2)	S2−C3	1.782(3)
Ru−N2	2.124(2)	S2−C4	1.781(3)
Cl1−Ru−Cl2	88.89(2)	Ru−S1−C2	113.7(1)
Cl1−Ru−S1	93.27(2)	O1−S1−C1	105.7(2)
Cl1−Ru−S2	87.70(2)	O1−S1−C2	106.1(1)
Cl1−Ru−N1	176.20(6)	C1−S1−C2	98.4(2)
Cl1−Ru−N2	87.29(5)	Ru−S2−O2	120.15(8)
Cl2−Ru−S1	89.95(2)	Ru−S2−C3	113.7(1)
Cl2−Ru−S2	174.96(3)	Ru−S2−C4	111.1(1)
Cl2−Ru−N1	88.07(5)	O2−S2−C3	105.3(1)
Cl2−Ru−N2	86.32(5)	O2−S2−C4	105.3(1)
S1−Ru−S2	93.95(2)	C3−S2−C4	98.9(2)
S1−Ru−N1	89.01(5)	Ru−N1−C5	120.6(2)
S1−Ru−N2	176.21(5)	Ru−N1−C9	122.7(2)
S2−Ru−N1	95.18(5)	C5−N1−C9	116.7(2)
S2−Ru−N2	89.91(5)	Ru−N2−C10	123.2(1)
N1−Ru−N2	90.23(7)	Ru−N2−C19	131.4(1)
Ru−S1−O1	117.28(9)	C10−N2−C19	105.0(2)
Ru−S1−C1	113.8(1)		

Starting Materials. Me_3Bzm was prepared as previously reported.[39] *cis*-$RuX_2(Me_2SO)_4$ (X = Cl, Br) were prepared by known methods.[40] Deuterated *cis*-$RuCl_2(Me_2SO)_4$ was obtained by dissolving the complex in warm DMSO-d_6 (0.5 g in 3 mL, 30 min); addition of acetone induced precipitation of the product.

***cis,cis,cis*-$RuCl_2(Me_2SO)_2(py)(Me_3Bzm)$ (1).** The complex could be synthesized by treating either *cis,fac*-$RuCl_2(Me_2SO)_3(py)$ or *cis,*-

(37) *MolEN. An Interactive Intelligent System for Crystal Structure Analysis*; Enraf-Nonius: Delft, The Netherlands, 1990.
(38) *International Tables for X-Ray Crystallography*; Kynoch Press: Birmingham, U.K., 1974; Vol. IV.
(39) Simonov, A. M.; Pozharskii, A. E.; Marianovskii, V. M. *Indian J. Chem.* **1967**, *5*, 81.
(40) Alessio, E.; Mestroni, G.; Nardin, G.; Attia, W. M.; Calligaris, M.; Sava, G.; Zorzet, S. *Inorg. Chem.* **1988**, *27*, 4099.

fac-$RuCl_2(Me_2SO)_3(Me_3Bzm)$ (*vide infra*) with a stoichiometric amount of the corresponding nitrogen ligand in ethanol at reflux (0.3 mmol of complex in 10 mL of ethanol; 1.5 h). The product slowly precipitated from the concentrated solution (1 mL) after addition of diethyl ether (~5 mL). It was then collected, washed with diethyl ether, and vacuum-dried at 25 °C (yield 30%). As shown by NMR (*vide infra*), the same geometrical isomer was obtained in both cases. If impurities such as *cis,cis,cis*-$RuCl_2(Me_2SO)_2(Me_3Bzm)_2$ and *trans,cis,cis*-$RuCl_2(Me_2SO)_2(py)_2$ were observed, **1** was recrystallized from chloroform/DMSO mixtures (50:1) after addition of diethyl ether (yield 65%). Anal. Calcd for $C_{19}H_{29}Cl_2N_3O_2RuS_2$ (MW 567.55): C, 40.21; H, 5.15; N, 7.40; S, 11.29; Cl, 12.49. Found: C, 40.33; H, 5.20; N, 7.25; S, 11.13; Cl, 12.35.

S-bonding was confirmed by IR data which showed strong S=O stretching bands (s = strong and m = medium): 1097, 1075 cm^{-1} (s, $\nu_{S=O}$ S-bonded); 421 cm^{-1} (m, ν_{Ru-S}).

***cis,cis,cis*-$RuCl_2(Me_2SO)_2(Me_3Bzm)_2$ (2).** In a typical preparation, Me_3Bzm (0.20 g, 1.25 mmol) was added to a suspension of *cis*-$RuCl_2(Me_2SO)_4$ (0.25 g, 0.5 mmol) in absolute ethanol (20 mL). The magnetically stirred mixture was then heated at reflux for 1.5 h. The mixture converted readily to a yellow solution that became a deep yellow. The volume was reduced *in vacuo* to ~4 mL. The yellow microcrystalline product, which rapidly precipitated from the solution, was collected after a few hours, washed with a small amount of cold ethanol and diethyl ether, and then vacuum-dried at 25 °C (yield 0.23 g, 70%). The complex was recrystallized from acetone/DMSO mixtures (15:1) after addition of diethyl ether (yield 80%). Anal. Calcd for $C_{24}H_{36}Cl_2N_4O_2RuS_2$ (MW 648.67): C, 44.44; H, 5.59; N, 8.63; S, 9.88; Cl, 10.93. Found: C, 44.50; H, 5.63; N, 8.59; S, 9.83; Cl, 10.83.

S-bonding was confirmed by IR data: 1109, 1087 cm^{-1} (s, $\nu_{S=O}$ S-bonded); 423 cm^{-1} (m, ν_{Ru-S}).

***cis,cis,cis*-$RuBr_2(Me_2SO)_2(Me_3Bzm)_2$ (3).** A procedure similar to that for **2** was used with *cis*-$RuBr_2(Me_2SO)_4$ as the starting material (yield 70%). Anal. Calcd for $C_{24}H_{36}Br_2N_4O_2RuS_2$ (MW 737.57): C, 39.08; H, 4.92; N, 7.59; S, 8.69; Br, 21.66. Found: C, 39.20; H, 5.04; N, 7.51; S, 8.61; Br, 21.84.

***cis,fac*-$RuCl_2(Me_2SO)_3(Me_3Bzm)$ (4).** Me_3Bzm (0.16 g, 1 mmol) was added to a magnetically stirred suspension of *cis*-$RuCl_2(Me_2SO)_4$ (0.25 g, 0.5 mmol) in methanol (8 mL). Within 15 min, the starting material dissolved completely, yielding a yellow solution, from which the product spontaneously precipitated. The reaction mixture was stirred for a total of 1 h. The product was collected, washed with cold methanol and diethyl ether, and then vacuum-dried at 25 °C. (yield 0.25 g, 85%). Anal. Calcd for $C_{16}H_{30}Cl_2N_2O_3RuS_3$ (MW 566.58): C, 33.92; H, 5.33; N, 4.94; S, 16.97; Cl, 12.51. Found: C, 33.80; H, 5.34; N, 4.92; S, 16.90; Cl, 12.41.

***cis,fac*-$RuCl_2(Me_2SO)_3(py)$ (5).** Py (80 μL, 1 mmol) was added to a magnetically stirred suspension of *cis*-$RuCl_2(Me_2SO)_4$ (0.25 g, 0.5 mmol) in methanol (8 mL). After 15 min, a yellow product precipitated from solution. The reaction mixture was stirred for another 45 min. The product was collected, washed with cold methanol and diethyl ether, and then vacuum-dried at 25 °C (yield 0.2 g, 80%). Anal. Calcd for $C_{11}H_{23}Cl_2NO_3RuS_3$ (MW 485.46): C, 27.21; H, 4.77; N, 2.88; S, 19.81; Cl, 14.60. Found: C, 27.20; H, 4.79; N, 2.85; S, 19.72; Cl, 14.51.

Results and Discussion

Synthesis. As reported for other nitrogen ligands,[34] the reaction between *cis*-$RuCl_2(Me_2SO)_4$ and either py or Me_3Bzm (L) in methanol at ambient temperature gave the poorly soluble monosubstituted derivatives of the general formula *cis,fac*-$RuCl_2(Me_2SO)_3L$. Precipitation precludes further reaction after replacement only of the more labile oxygen-bonded Me_2SO.[34] The three facially oriented Me_2SO ligands are bound through sulfur rather than oxygen. This was confirmed by IR data which showed strong S=O stretching bands (s = strong, m = medium, and br = broad). *cis,fac*-$RuCl_2(Me_2SO)_3(Me_3Bzm)$ (**4**): 1094 cm^{-1} (s, br, $\nu_{S=O}$ S-bonded); 425 cm^{-1} (m, ν_{Ru-S}). *cis,fac*-$RuCl_2(Me_2SO)_3(py)$ (**5**): 1103, 1083 cm^{-1} (s, $\nu_{S=O}$ S-bonded); 425 cm^{-1} (m, ν_{Ru-S}).

Table 4. ^1H NMR Chemical Shifts (ppm) of *cis,fac*-$RuCl_2(Me_2SO)_3L$ (L = Me_3Bzm (**4**), py (**5**)) in $CDCl_3$[a,b]

	L	
	Me_3Bzm	py
B2H/α-H	8.82	9.11 (d)
B4H/β-H	7.87	7.33 (t)
B7H/γ-H	7.21	7.78 (t)
$B10H_3$	2.39	
$B11H_3$	2.39	
$B12H_3$	3.87	
Me_2SO	3.50	3.53
	3.30	3.52
	3.24	3.30

[a] See Chart 1 for Me_3Bzm notation. [b] d = doublet; t = triplet.

Chart 2. Labeling Scheme for the Octahedral Ru Complex Ligand Positions

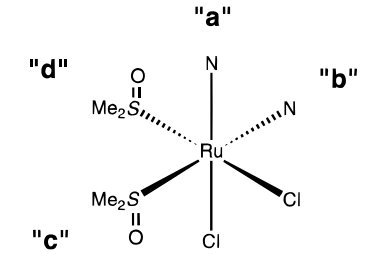

The ^1H NMR spectra of **4** and **5** are as expected for a *cis,fac* geometry.[34,41,42] The spectra of $RuCl_2(Me_2SO)_3L$ (L = py, Me_3Bzm) (Table 4) contain three signals of equal intensity in the S-bonded Me_2SO region (3.20−3.60 ppm), a singlet, and two unresolved quartets. The sharp singlet is due to the equivalent methyl groups of the Me_2SO *trans* to L, while the slightly broader signals are attributed to the two enantiotopic pairs of diastereotopic methyl groups[43] on the equivalent Me_2SO ligands *trans* to Cl. They appear as poorly resolved quartets due to $^1H-^1H$ coupling between diastereotopic methyls on the same Me_2SO. A *cis,mer*-$RuCl_2(Me_2SO)_3L$ derivative should give a similar NMR pattern, but the rearrangement of the three Me_2SO ligands would very likely induce a significant change (not observed) in the UV−visible spectrum compared to that of the precursor. Furthermore, the spectra of **4** (λ_{max} 351 nm, ϵ 410) and **5** (λ_{max} 341 nm, ϵ 720) are similar to those of derivatives of known structure such as *cis,fac*-$RuCl_2(Me_2SO)_3NH_3$ (λ_{max} 351 nm, ϵ 321).[34] Moreover, the formation of such a *cis,mer* isomer is not expected from the known reactivity of *cis*-$RuCl_2(Me_2SO)_4$. Two sharp singlets in a 1:2 ratio would be expected if the $RuCl_2(Me_2SO)_3L$ geometry were *trans*. Therefore, we are confident that **4** and **5** have the *cis,fac* geometry.

Symmetrically disubstituted compounds, *cis,cis,cis*-$RuCl_2(Me_2SO)_2L_2$, can also be obtained by direct reaction of *cis*-$RuCl_2(Me_2SO)_4$ with 2 equiv of nitrogen ligand L in ethanol at reflux.[34] Treatment of *cis,fac*-$RuCl_2(Me_2SO)_3L$ precipitates with a stoichiometric amount of another nitrogen ligand (L′) in ethanol at reflux produced mainly *cis,cis,cis*-$RuCl_2(Me_2SO)_2LL'$ derivatives. Two different *cis,cis,cis*-geometric isomers might be expected when L is different from L′ since L could be *trans* to either Cl (position "a") or Me_2SO (position "b") (Chart 2).

***cis,cis,cis*-$RuCl_2(Me_2SO)_2(py)(Me_3Bzm)$ (1).** From the procedure just described, only one *cis,cis,cis*-$RuCl_2(Me_2SO)_2(py)(Me_3$-

(41) Barnes, J. R.; Goggin, P. L.; Goodfellow, R. J. *J. Chem. Res., Miniprint* **1979**, 1610.
(42) Barnes, J. R.; Goodfellow, R. J. *J. Chem. Res., Miniprint* **1979**, 4301.
(43) Mestroni, G.; Alessio, E.; Zassinovich, G.; Marzilli, L. G. *Comments Inorg. Chem.* **1991**, *12*, 67.

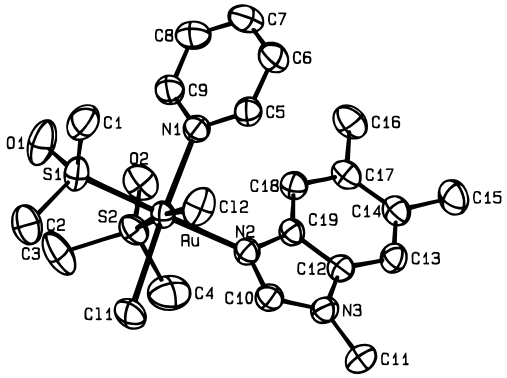

Figure 1. Perspective drawing and labeling scheme for the non-hydrogen atoms of *cis,cis,cis*-$RuCl_2(DMSO)_2(py)(Me_3Bzm)$ (**1**).

Table 5. ^1H NMR Chemical Shifts (ppm) of *cis,cis,cis*-$RuCl_2(Me_2SO)_2(py)(Me_3Bzm)$ (**1**) in $CDCl_3$[a,b]

α-H	9.52 (b)	8.44 (b)
β-H	7.35 (b)	6.78 (b)
γ-H	7.62 (t)	
B2H	8.79	
B4H	6.22	
B7H	7.17	
$B10H_3$	1.95	
$B11H_3$	2.31	
$B12H_3$	3.90	
	"c"	"d"
Me_2SO	3.49	3.74
	2.90	2.69

[a] See Chart 1 for Me_3Bzm notation. [b] b = broad; t = triplet.

Bzm) geometrical isomer was isolated after concentration of solutions of py added to **4** or Me_3Bzm added to **5**. Furthermore, this same complex was obtained from *cis*-$RuCl_2(Me_2SO)_4$ treated with 1:1 py:Me_3Bzm mixtures. No NMR evidence of the other geometrical isomer was found in any case. Since Me_3-Bzm and py have similar donor abilities, this result indicates that the product formed is thermodynamically controlled and suggests that there might be a steric basis for the selectivity.

The compound was subjected to single-crystal X-ray analysis. As shown in Figure 1, the Cl, Me_2SO, and N ligands all occupy *cis* positions, with py *trans* to Cl (position "a") and Me_3Bzm *trans* to Me_2SO (position "b") (Chart 2). Furthermore, the plane of the py ring (coplanar within 0.012 Å) lies between the two S atoms, with S1 and S2 1.676 and −1.602 Å, respectively, out of the plane. The plane of the Me_3Bzm ring (coplanar within 0.054 Å) is oriented with the head, represented by C10 (B2), pointing toward the Cl atoms; but in this case C10 is not symmetrically placed with respect to the Cl atoms (Cl1 −0.962 Å and Cl2 2.300 Å out of the plane). In contrast, the H18 on C10 (B2H in the NMR tables) is closer to being equidistant from the two Cl atoms (H18−Cl1, 2.69 Å; H18−Cl2, 3.15 Å). The planes of the two N ligands form a dihedral angle of 49.2°. Interestingly, the Ru−N2−C19 bond angle is 131.4(1)° (Table 3); normally an ∼133° angle is found for M−BN3−B9.[44−46]

Because of the lack of symmetry of **1**, its ^1H NMR spectrum (Table 5) has seven sharp singlets in the methyl region, corresponding to the four diastereotopic Me_2SO methyl groups and the three Me_3Bzm methyl groups. In the aromatic region, while the Me_3Bzm and the B2H, B4H, and B7H signals are

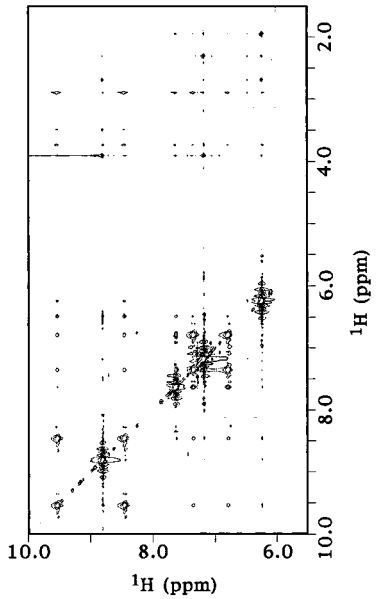

Figure 2. 2D ^1H homonuclear ROESY spectrum of *cis,cis,cis*-$RuCl_2(Me_2SO)_2(py)(Me_3Bzm)$ (**1**) in the downfield region.

sharp, the py α and *β* protons give four well-resolved but relatively broad resonances. This pattern is attributed to a slow-to-intermediate rotation rate of py about the Ru−N bond on the NMR time scale. All five py protons are in fact magnetically inequivalent. However, rotation about the Ru−N bond will physically exchange the chemically equivalent protons (α and α′, *β* and *β*′). The *γ* proton gives a well-resolved triplet since it lies on the rotation axis.

ROESY data for **1** show strong negative exchange cross-peaks between each pair of chemically equivalent py protons (Figure 2), confirming that they are exchanged by rotation about the Ru−N bond. The ROESY spectrum also has rather strong intraligand positive NOE cross-peaks between protons bound to adjacent ring carbon atoms (α → *β* → *γ*) and between methyl groups on the same Me_2SO. Initial identification of the Me_2SO peaks was achieved through the synthesis of the DMSO-d_6 derivative. With the reasonable assumption that the most downfield Me_3Bzm methyl signal is the NCH_3 ($B12H_3$ at 3.90 ppm), the NOE connectivities (Chart 1) allowed complete assignment of the Me_3Bzm signals (Table 5). $B12H_3$ has NOE cross-peaks to B2H and B7H, distinguished by the B7H−$B11H_3$ NOE cross-peak. All the py signals have interligand NOE cross-peaks with signals of both Me_2SO ligands in the ROESY spectrum; py must be *cis* to both Me_2SO ligands (position "a"). The Me_3Bzm ligand, on the other hand, shows significant cross-peaks with only one Me_2SO ligand. As expected from the *cis* relationship and from the solid state structure, the α-H's have NOEs to B4H and *γ*-H has an NOE to $B10H_3$. Because of the py rotation, the α-H NOEs are comparable and we cannot use NOE cross-peaks to assign a particular α-H signal to a given α-H in relation to the solid state structure. However, we believe that the upfield α-H and *β*-H signals are due to the H's on C5 and C6, respectively, in the X-ray structure, since these protons are in the shielding cone of Me_3Bzm.

A variable-temperature NMR study showed that the spectrum of *cis,cis,cis*-$RuCl_2(Me_2SO)_2(py)(Me_3Bzm)$ is substantially unchanged between +20 and −80 °C, except for the expected sharpening of the py α-H and *β*-H peaks as the rotation rate of the ligand became slow on the NMR time scale. The α-H resonances appear as doublets and the *β*-H signals as pseudo-triplets for temperatures below −40 °C. This means that at low temperature (below −40 °C) the complex exists in solution

(44) Parker, W. O., Jr.; Zangrando, E.; Bresciani-Pahor, N.; Marzilli, P. A.; Randaccio, L.; Marzilli, L. G. *Inorg. Chem.* **1988**, *27*, 2170.
(45) Charland, J.-P.; Zangrando, E.; Bresciani-Pahor, N.; Randaccio, L.; Marzilli, L. G. *Inorg. Chem.* **1993**, *32*, 4256.
(46) Charland, J.-P.; Attia, W. M.; Randaccio, L.; Marzilli, L. G. *Organometallics* **1990**, *9*, 1367.

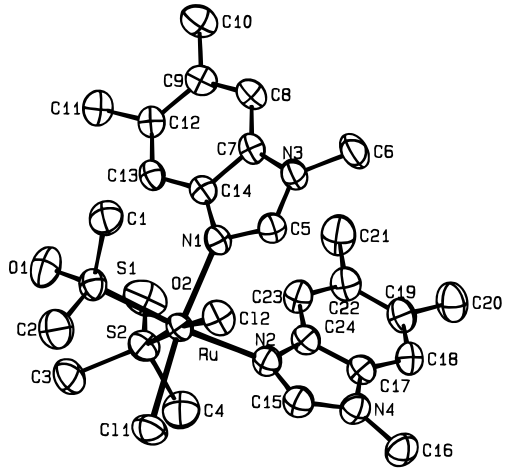

Figure 3. Perspective drawing and labeling scheme for the nonhydrogen atoms of *cis,cis,cis*-$RuCl_2(Me_2SO)_2(Me_3Bzm)_2$ (**2**).

as a pair of degenerate rotamers (topomers)[20,21] in which py assumes two positions 180° relative to each other. Rotamers differing by torsion angles other than 180° would not be degenerate, since each orientation of py would induce a different local magnetic field on the other ligands. A splitting of all the peaks would be expected in case of such nondegenerate rotamers (diastereotopomers), but such splitting was not seen in this case.

The ^{1}H NMR spectrum of **1** does provide some conclusive information about the motion of the Me_3Bzm "b" in **2** (*vide infra*). The results for **2** are consistent with one of the following hypotheses for the Me_3Bzm "b": (i) it is always in fast rotation on the NMR time scale, (ii) it is in a fixed position over the whole temperature range examined, or (iii) it rotates synchronously with the *cis* heterocyclic ligand. In all cases, only one set of signals is expected for this Me_3Bzm "b" for **2**. For **1**, slow synchronous rotation on the NMR time scale of the lopsided ligand between any two orientations would generate two sets of signals for every ligand, since two diastereotopomers would be formed. Thus, for example, there would be four α-H signals observed. This result was not found, and therefore hypothesis iii can be ruled out. In addition, if Me_3Bzm "b" were in fast rotation, the slower rotation at lower temperature could lead to some line broadening. The absence of line broadening and the other results for **1** strongly support hypothesis ii.

***cis,cis,cis*-$RuCl_2(Me_2SO)_2(Me_3Bzm)_2$ (2).** The most interesting feature of the molecular structure of **2** (Figure 3)[22] is the head-to-head (HH) arrangement of the two Me_3Bzm ligands, both B2H's being on the same side of the equatorial N1−N2−Cl1−S1 plane. The Me_3Bzm in position "a" (coordinated by N1, coplanar within 0.020 Å) is oriented in such a way as to bisect the S1−Ru−S2 angle (S1 1.532 Å and S2 −1.726 Å out of the plane); consequently, Cl2 is close (2.66 Å) to H13 on C5 (B2H "a" in the NMR labeling scheme below). In contrast, the Me_3Bzm in position "b" (coordinated by N2, coplanar within 0.013 Å) approximately bisects the Cl1−Ru−Cl2 angle (Cl1 −1.23 Å and Cl2 2.09 Å out of the plane), so that H25 on C15 (B2H "b") is nearly equidistant from the two Cl atoms (H25−Cl1, 2.95 Å; H25−Cl2, 3.08 Å). The two planes are inclined at 47.7°. The Ru−N1−C14 (B9) bond angle is highly distorted from trigonal geometry up to 135.9(1)°,[22] most likely due to the steric interactions of the six-membered ring of Me_3Bzm "a" with the two *cis* Me_2SO ligands. The chemically equivalent Ru−N2−C24 (B9) bond angle of 128.5(2)° appears to be much less distorted; Me_3Bzm "b" interacts only with one Me_2SO group. The slightly longer Ru−N bond distance for "b" (2.139(2) Å) compared to that for "a" (2.115(2) Å) can be attributed to the *trans* influence of Me_2SO.[47] This longer bond may contribute somewhat to the lower steric demands of site "b".

Table 6. ^{1}H NMR Chemical Shifts (ppm) of *cis,cis,cis*-$RuCl_2(Me_2SO)_2(Me_3Bzm)_2$ (**2**) and *cis,cis,cis*-$RuBr_2(Me_2SO)_2(Me_3Bzm)_2$ (**3**) in $CDCl_3$[a]

	I		II	
	Cl	Br	Cl	Br
		Me_3Bzm "a"		
B2H	8.70	8.73	7.43	7.55
B4H	6.73	6.70	8.25	8.28
B7H	6.92	6.92	7.06	7.06
$B10H_3$	1.71	1.68	2.48	2.47
$B11H_3$	2.11	2.10	2.41	2.41
$B12H_3$	3.90	3.89	3.36	3.33
		Me_3Bzm "b"		
B2H	8.92	9.17	8.90	9.15
B4H	6.07	6.06	6.11	6.07
B7H	7.04	7.03	7.17	7.17
$B10H_3$	1.70	1.67	1.85	1.83
$B11H_3$	2.16	2.15	2.31	2.31
$B12H_3$	3.95	3.95	3.92	3.92
		Me_2SO "c"		
$(CH_3)_1$	3.49	3.68	3.55	3.77
$(CH_3)_2$	3.01	3.18	2.86	3.02
		Me_2SO "d"		
$(CH_3)_1$	3.78	3.91	3.78	3.91
$(CH_3)_2$	2.80	2.88	2.57	2.65

[a] See Chart 1 for Me_3Bzm notation and Chart 2 for ligand positions.

Since all the ligands in **2** are inequivalent, its ^{1}H NMR spectrum would be expected to have six aromatic signals and ten methyl signals. However, the spectrum in $CDCl_3$ has twice the expected number of peaks (see the 1D spectra shown on the axes in supplementary 2D NMR figures), strongly suggesting the presence of two rotamers that interconvert slowly on the NMR time scale (due to the lopsided nature of the ligand, only nondegenerate pairs of rotamers, diastereotopomers, will be possible in this case). One of the rotamers (I) is slightly less abundant than the other (II) (45:55 ratio from peak integration), allowing the signals in the 1D spectrum to be easily divided into two sets according to their intensity; each peak in the less intense set (I) relates via an EXSY cross-peak to a peak in the other set (II). A similar ratio between the two rotamers was measured in other solvents, such as CD_2Cl_2, CD_3COCD_3, and DMSO-d_6.

A complete assignment of the 16 peaks of each rotamer (Table 6) was performed according to the following steps: (i) Synthesis of the DMSO-d_6 derivative allowed assignment of the Me_2SO methyl signals. (ii) As in the case of **1** reported above, rather strong intraligand NOE cross-peaks were detected in the ROESY spectrum. The NOE connectivity paths allowed designation of the signals belonging to each one of the two Me_3Bzm ligands ("a" and "b") and to the two Me_2SO ligands ("c" and "d") in each rotamer. (iii) With the same strategy used for **1**, the signals of each Me_3Bzm were unambiguously assigned (Table 6). Since the assignment was intricate, it is described in the Supporting Information. The final assignment of the Me_3Bzm ligand positions (Chart 2) was accomplished by interligand NOE interactions in ROESY and 1D NOE spectra. In particular, Me_2SO "d" was the only Me_2SO ligand to show cross-peaks with H2 and H4 of both Me_3Bzm ligands, unambiguously demonstrating that it is *cis* to both. On the other hand, Me_2SO "c" gave cross-peaks only with H2 and H4 protons of Me_3Bzm "a", implying that the two ligands must be *cis* to each other.

(47) Calligaris, M.; Carugo, O. *Coord. Chem. Rev.*, in press.

These relationships allow the positions of the ligands to be determined unambiguously. The chemical shifts of Me_3Bzm "b" in **2** are rather close to those of Me_3Bzm "b" in **1** (*cf.* Tables 5 and 6), suggesting that the anisotropic effects on "b" of the two different aromatic ligands in position "a" are similar.

The assignments determined on the basis of the above NOE arguments also agree with those obtained by comparing the chemical shifts of *cis,cis,cis*-$RuCl_2(Me_2SO)_2(Me_3Bzm)_2$ (**2**) and *cis,cis,cis*-$RuBr_2(Me_2SO)_2(Me_3Bzm)_2$ (**3**). These analogues must be closely related in structure since the ratio between the two rotamers is essentially the same in **2** and **3**. In metal−halide−Me_2SO complexes, substitution of a chloride with a bromide induces a downfield shift of the Me_2SO signals, with signals of Me_2SO ligands *cis* to the halide affected more than those *trans* to it.[41,42] The methyl signals of Me_2SO "c" are shifted much more downfield than those of the other Me_2SO ("d") in **3** than in **2** (Table 6). This result suggests that "c" is *cis* to two halides and "b" is *cis* to only one halide. If signals of Me_3Bzm ligands can be affected as those of Me_2SO by the nature of the halides, Me_3Bzm "b" is *cis* to two halides and "a" is *cis* to only one halide.; hence, "b" and "c" must be *trans* to each other.

With the ligand positions assigned, we turn to the determination of which of the four possible atropisomers are formed. The chemical shifts of Me_3Bzm "a" are considerably more dispersed than those of "b" (Table 6), suggesting that Me_3Bzm "a" protons experience remarkably different magnetic environments in the two rotamers. This feature of ligand "a" is most evident for the B2H and B4H signals. For example, in II, B4H "a" is actually more downfield than B2H "a". Such large effects indicate that Me_3Bzm "a" is flipping between two quite different orientations, while the other nitrogen ligand "b" is either in a fixed position or in free rotation. Observe that in *cis,cis,cis*-$RuCl_2(Me_2SO)_2(py)(Me_3Bzm)$ the ligand undergoing rather slow rotation, py, is the one in position "a".

The Me_3Bzm ligand in *cis,fac*-$RuCl_2(Me_2SO)_3(Me_3Bzm)$ can be used as a reference for the evaluation of the effects of the ligand "a" on the chemical shifts of Me_3Bzm in position "b" (*cf.* Tables 4−6). Substitution of Me_2SO in position "a" (Chart 2) with either py (**1**) or Me_3Bzm (**2**) does not affect significantly the chemical shifts of B2H and $B12H_3$ of Me_3Bzm "b". Therefore, the shifts of these protons might be mainly influenced by the coordination of Me_3Bzm to the Ru(II) nucleus and by the proximity of the two halides. On the contrary, "b" B4H is dramatically shifted upfield upon introduction of an aromatic ligand "a", strongly suggesting that in both **1** and **2**, this proton might fall into the shielding cone of "a". Likewise, "b" $B10H_3$ and, to a lesser extent, "b" $B11H_3$ have shifted upfield. If Me_3Bzm "b" in **2** remains in a fixed position with the orientation found in the solid, its six-membered ring is positioned over the shielding cone of "a" in both rotamers. The influence of Me_3Bzm "b" on the chemical shifts of the ligand in "a" is more difficult to evaluate due to the lack of a model. However, if we assume that normal shifts for $B10H_3$ and $B11H_3$ are ∼2.4 ppm (Co(III) complexes[44−46]), then $B10H_3$ and $B11H_3$ are upfield shifted in **2** except for Me_3Bzm "a" in II. The upfield shift of B2H and $B12H_3$ of Me_3Bzm "a" in II can be attributed to their positions in the shielding cone of Me_3Bzm "b".

According to the above arguments, the HH conformer frozen in the crystal structure of **2** (Figure 3)[22] is most likely the structure of the more abundant rotamer, II. This would be in agreement with the hypothesis (posed above) that the downfield chemical shift of "b" B2H II is due mainly to its proximity to the halides. The upfield shift of "a" B2H II is due to its proximity to the shielding cone of "b" despite its closeness to the *cis* chloride. The downfield shift of "a" B4H II is likely due to its deshielding by "b". Several other shift relationships are explained readily if II is HH and I is HT.

On the basis of the crystal structure H−H interatomic distances, some interligand NOE signals found for II in the ROESY spectrum between "a" B2H and "b" B4H (3.60 Å), "c" $(CH_3)2$ (methyl group C1 in crystal structure, methyl group 2 of Me_2SO "c" in NMR notation) and "a" B4H (4.16 Å), and "d" $(CH_3)2$ (methyl group C4 in crystal structure, methyl group 2 of Me_2SO "d" in NMR notation) and "b" B4H (3.72 Å) are among those expected. Although no solid state structure is available for the HT species, I, the orientation of the two *cis* bases in I would place B4H "a" in close proximity to B2H "b" and B4H "b" close to B2H "a". As expected, the ROESY spectrum reveals these NOEs. In addition, NOEs are present between B2H "a" and Me_2SO signals of "c" and "d" orienting the head of ligand "a" toward the Me_2SO ligands. B4H "b" has expected NOEs to ligand "d" (head toward the halides).

A variable-temperature study showed that the ^1H NMR spectrum of **2** is essentially unchanged between −100 and +35 °C, the rate of conformational equilibrium remaining in the slow-exchange limit. The exchange process observed in the ^1H NMR spectrum of *cis,cis,cis*-$RuCl_2(Me_2SO)_2(Me_3Bzm)_2$ involves at least one nitrogen ligand in slow rotation on the NMR time scale between two orientations. (Four sets of signals would be expected if both nitrogen ligands were in independent slow rotation between two positions.) The three hypotheses considered above for **1** can explain the behavior of the second nitrogen ligand in **2**. From the results for **1**, it is reasonable to exclude synchronous rotation and to assume that Me_3Bzm "a" is rotating and that Me_3Bzm "b" either (i) is in fast rotation or (ii) remains in a fixed position. Again as for **1**, the signals of Me_3Bzm "b" do not broaden on lowering the temperature, strongly supporting hypothesis ii. We also excluded the possibility that Me_3Bzm was changing its orientation by dissociation/reassociation. Using selective irradiation, we established that in a solution of **2** and free Me_3Bzm there was no ligand exchange on the NMR time scale.

How can all the observations be rationalized? We believe the following three factors can be used: the stronger attractive electrostatic interaction for the *cis* halide of the electron-deficient B2H compared to B4H or the py α-H, the more crowded nature of site "a" compared to site "b", and the larger bulk of Me_3Bzm compared to py.

If site "a" is sterically more demanding and py has smaller bulk, then the occupation of site "a" by py and site "b" by Me_3Bzm in **1** can be readily understood. Some structural evidence that site "a" is constrained can be found in the large distortions of Ru−N−C bond angles for Me_3Bzm "a" in **2**. Despite this apparent steric repulsion, the HH rotamer has stability comparable to that of the HT rotamer, which models suggest has fewer unfavorable steric interactions. We believe the steric repulsions of Me_3Bzm "a" in the HH rotamer are offset to some extent by the electrostatic attraction for the *cis* chloride of the electron-deficient B2H.

In contrast to site "a", which has three bulky *cis* ligands, site "b" has only two bulky *cis* ligands. In the preferred orientation, the six-membered ring of Me_3Bzm "b" is directed toward these bulky ligands. Here the Ru−N−C angles are smaller, consistent with the lower steric constraints of site "b". Furthermore, the electron-deficient B2H of Me_3Bzm "b" can interact with two *cis* chlorides. Therefore, it is possible that the orientation of Me_3Bzm "b" found in the solid and solution states for both **1** and **2** is especially favored. In this way the relative stability of the observed rotamers can be rationalized.

The rotation rates depend on the size of the activation barriers. Since ligand "a" occupies the more crowded site (and hence less stable site) and Me_3Bzm "b" the less crowded (more stable) site in the ground state species, the barrier to rotation may be lower for ligand "a" than for Me_3Bzm "b" in both **1** and **2**. The increase in the distance between the $\delta+$ H and the two *cis* Cl ligands accompanying any rotation of Me_3Bzm "b" will decrease the favorable electrostatic attraction between these charged groups. This decrease will make rotation of Me_3Bzm "b" less favorable. The faster rotation rate of py "a" in **1** vs Me_3Bzm "a" in **2** can be attributed to the smaller bulk of py.

Conclusions

Compound **2** holds the distinction of being the first compound of its type found to be HH both in solution and in the solid state. We have clearly established that the HH form is in equilibrium with a HT form in solution; we have provided very strong evidence that atropisomerization involves rotation of Me_3Bzm "a" and Me_3Bzm "b" remains relatively fixed. In the HH rotamer, Me_3Bzm "a" remains canted in solution, with B2H pointed toward Me_3Bzm "b". The factors favoring this canting and the orientation of Me_3Bzm are not completely clear. Nevertheless, our results suggest that the orientation can be rationalized as resulting from a balance between the steric interactions of the bulky six-membered-ring portion of Me_3Bzm with the bulkier ligands (Me_2SO and Me_3Bzm) and an electrostatic attraction of the $\delta+$ B2H toward the Cl ligands.

Cis bis complexes of lopsided ligands are very important in metal systems of biological importance. In purine complexes, the HH orientation is rare, and relatively little information exists on the mutual effects of imidazole ligands in metalloproteins and metalloenzymes. Understanding the fundamental factors that influence both the structural and dynamic properties of *cis* bis complexes of lopsided ligands is essential to the elucidation of the role of such metal complexes in biological systems. In metalloproteins, the metal center frequently has a mixed-ligand environment composed of coordinated negative ligands (carboxylates, thiolates) and imidazoles. The relative orientation of the imidazoles may be influenced not only by the demands of the protein but also by the steric/electrostatic interactions within the coordination environment such as outlined here. Additional systems must be studied to gain a clearer insight into the mutual effects on orientation of heterocycles and into other interligand interactions influencing orientation.

Acknowledgment. We thank the NIH (Grant GM 29222) for support, NATO for a fellowship to E.A., and Johnson Matthey for a loan of $RuCl_3$. The instrument purchases were funded by the NIH and NSF. L.G.M. was supported in part by Emory's F. M. Bird Exchange Fellowship to St. Andrews University, Scotland.

Supporting Information Available: Text giving assignments of the NMR signals for *cis*,*cis*,*cis*-$RuCl_2(Me_2SO)_2(Me_3Bzm)_2$, 2D NMR spectra used for assignment of the NMR signals for **2**, and tables of complete bond distances and angles, general displacement parameter expressions B (Å^2), and positional and thermal parameters of hydrogen atoms for **1** (11 pages). Ordering information is given on any current masthead page.

IC9509793